# Evidence for a Double Well in the First Triplet Excited State of 2-Thiouracil

Daisuke Koyama, Matthew J. Milner and Andrew J. Orr-Ewing*

*School of Chemistry, University of Bristol, Cantock's Close, Bristol BS8 1TS, UK*

12 September 2017

* Author for Correspondence

Tel: +44 (0)117 9287672

e-mail: A.Orr-Ewing@bristol.ac.uk

ABSTRACT

The computationally predicted presence of two structurally distinct minima in the first triplet excited ($T_1$) state of 2-thiouracil (2TU) is substantiated by sub-picosecond transient vibrational absorption spectroscopy (TVAS) in deuterated acetonitrile solution. Following 300-nm ultraviolet excitation to the second singlet excited state of 2TU, a transient infrared absorption band centered at 1643 $cm^{-1}$ is observed within our minimum time resolution of 0.3 ps. It is assigned either to 2TU molecules in the $S_1$ state, or to vibrationally hot $T_1$ state molecules, with the latter assignment more consistent with recent computational and experimental studies. The 1643 $cm^{-1}$ band decays with a time constant of 7.2 ± 0.8 ps, and there is corresponding growth of several further bands centered at 1234, 1410, 1424, 1443, 1511, 1626 and 1660 $cm^{-1}$ which show no decline in intensity over the 1 ns time limit of our measurements. These spectral features are assigned to two different conformations of 2TU, corresponding to separate energy minima on the $T_1$ state potential energy surface, on the basis of their extended lifetimes, computed infra-red frequencies, and the observed quenching of the bands by addition of styrene. Corresponding measurements for the 4-thiouracil (4TU) isomer show sub-picosecond population of the $T_1$ state, which vibrationally cools with a time constant of 5.2 ± 0.6 ps. However, TVAS measurements in the carbonyl stretching region do not distinguish the two computed $T_1$-state conformers of 4TU because of the similarity of their vibrational frequencies.

## 1. INTRODUCTION

The five canonical nucleobases (cytosine, guanine, adenine, thymine, and uracil) form the majority of the functional core of nucleic acids and, through Watson-Crick base pairing, are the key to the transcription, translation and replication of the genetic code. One of the most remarkable features of nucleic acid photochemistry is the photostability of the canonical nucleobases.[1] These heterocyclic molecules have ultrafast relaxation pathways from excited singlet states to their ground states through conical intersection, which are considered to provide a primary defense against solar ultraviolet (UV) radiation damage.[2-3]

The five canonical nucleobases are the most commonly occurring in living organisms, but post-transcriptional modification gives rise to other nucleobases.[4] Transfer RNA (tRNA) is especially notable for its diverse range of nucleotides, and one modification prevalent in prokaryotic tRNA is thionation (i.e., a sulfur-oxygen substitution). The photochemical dynamics exhibited by thionucleobases depart significantly from those of their canonical analogues; in particular, the presence of a sulfur atom facilitates triplet state formation. The long-lived triplet states of thionucleobases can serve as photosensitizers for photochemotherapy.[5-7]

The photochemical dynamics of thionucleobases have been extensively studied both by experimental[8-17] and theoretical approaches,[18-26] with the aim of developing a fundamental understanding of the differences from the canonical nucleobases. These studies have recently been reviewed,[27-28] and the broad consensus from prior work is that ultrafast intersystem crossing (ISC) takes place in thionucleobases on timescale less than 1 ps, with almost unity quantum yield. For example, Crespo-Hernández and co-workers

studied several thionucleobases in the condensed phase using transient electronic absorption spectroscopy (TEAS) and reported sub-picosecond ISC dynamics.[9-10, 29] González and co-workers, and Persico and co-workers respectively investigated the photochemical relaxation pathways of 2-thiouracil (2TU) and 6-thioguanine using high level *ab initio* computational simulations, and identified mechanisms responsible for the ultrafast ISC.[20, 24]

Recently, Bai and Barbatti focused on discrepancies in the quantum yields for singlet oxygen generation by triplet energy transfer from thionucleobases.[25] Their computational study compared 2-thiothymine and 6-aza-2thiothymine, for which the singlet oxygen quantum yields were previously reported to be 0.36 and 0.69.[9, 13] They proposed that the differences in the singlet oxygen yields derive from the presence of a double well in the $T_1$ excited state. Singlet oxygen yields are governed by the $T_1$ state lifetimes, and they suggested that one of the two $T_1$ minima could access an intersection to the ground electronic state. The relative energies of the two minima therefore influence the efficiency of singlet oxygen production. The existence of two $T_1$ minima in 2TU was also computationally predicted by González and co-workers,[23] and has recently been invoked to explain the time-dependence of the decay of the $T_1$ state to the $S_0$ ground state.[17]

Here, we present experimental evidence for the population of two separate minima on the 2TU $T_1$-state potential energy surface (PES) upon photoexcitation. This evidence derives from transient vibrational absorption spectroscopy (TVAS) in the infra-red region of the spectrum, where bands are generally sharper than those recorded by TEAS.[30] We interpret the results with the aid of the prior sub-picosecond TEAS measurements, and

previous computational studies of the excited state PESs and non-adiabatic dynamics.[23-24, 29] We also report the photochemical dynamics of an isomer of 2TU, 4-thiouracil (4TU), observed by TVAS. These 4TU measurements assist with the interpretation of the TVA spectra of 2TU. The chemical structures of both compounds are illustrated below, together with the ring-atom numbering scheme used in our assignments of vibrational modes.

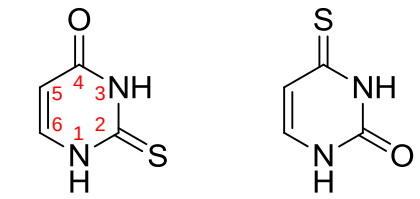


2-thiouracil (2TU) 4-thiouracil (4TU)

## 2. EXPERIMENTAL DETAILS

2-thiouracil (≥ 99%), 4-thiouracil (≥ 97%) and deuterated acetonitrile ($CD_3CN$, ≥ 99.8 atom % D) were purchased from Sigma Aldrich and used as received. TVAS measurements were carried out using an ultrafast laser system, the details of which have been reported elsewhere.[31-32] Briefly, each solution to be investigated was continuously circulated through a Harrick cell which enclosed the sample between two transparent $CaF_2$ windows separated by a 200-μm PTFE spacer. The infrared range probed spanned 1210 $cm^{-1}$ to 1760 $cm^{-1}$, with solvent bands obscuring transient signals to higher wavenumber (e.g. in the N-H stretching region). The UV excitation wavelength used was 300 nm for 2TU (unless otherwise specified) and 320 nm for 4TU with energies of 600 nJ / pulse. Steady state UV-vis absorption spectra are shown in Figure S1 of the Supporting Information. The vertical excitation from the ground state ($S_0$) to the first

singlet excited state ($S_1$) of the thionucleobases (which are examples of thiocarbonyl compounds) is a weak $\pi^* \leftarrow n$ transition. and the excitation wavelengths used in this study instead predominantly correspond to stronger transitions to the second singlet excited states ($S_2$) with $^1\pi\pi^*$ character in the Franck-Condon region.[14-15, 19, 23, 26, 29] The sample concentrations were 1.8 mM for both 2TU and 4TU / $CD_3CN$ solutions, corresponding to optical densities of ~0.5 at the chosen excitation wavelengths and sample pathlengths. At this concentration, intermolecular stacking is judged to be negligible from the linear dependence of absorbance on concentration (see Figure S2 for 2TU and S3 for 4TU). The ultrafast pump and probe instrument response function was 150 fs, determined from fitting the observed growth of a 2TU bleach band at 1705 $cm^{-1}$, but the minimum time delay for reliable spectra was limited to 300 fs by thermal lensing.[32]

Computational geometry optimizations and calculations of fundamental vibrational frequencies of 2TU and 4TU were performed using the Gaussian 09 program.[33] The calculations used the B3LYP density functional for the ground states and unrestricted B3LYP (UB3LYP) for the $T_1$ states,[34-35] with the 6-311++G(3df,3pd) basis set and the conductor polarizable continuum model (CPCM),[36-37] to take into account the electrostatic effects of the acetonitrile solvent. The resulting optimized geometries are presented in the Supporting Information. This method best reproduced steady-state FTIR spectra for 2TU (shown in Figure S2) from among our preliminary computational tests (see Table S1 of Supporting Information for details). The equilibrium geometries and vibrational frequencies for the $S_1$ state of 2TU were obtained using time-dependent density functional theory (TDDFT) at the B3LYP / 6-311+G(d,p) / CPCM (acetonitrile) level of theory. The accuracy of the computed $S_1$-state infrared frequencies was checked by comparison of vibrational frequencies for the $T_1$ state obtained by the same TDDFT

method with those predicted by the UB3LYP calculations (Table S2). No scaling factor was applied for correction of computed infrared frequencies.

## 3. RESULTS AND DISCUSSION

We begin with the photochemical relaxation dynamics of 4TU deduced from TVA spectra, followed by those of 2TU. The analysis of the 4TU spectra is more straightforward, and establishes a timescale for vibrational relaxation which contributes to the interpretation of the 2TU measurements.

### 3.1. Photochemical Relaxation Dynamics of 4-Thiouracil

Figure 1 shows TVA spectra of 1.8 mM 4TU in $CD_3CN$ solution following 320-nm excitation. The two negative bands at 1622 $cm^{-1}$ and 1739 $cm^{-1}$ derive from depletion of the ground state 4TU by the pump UV light, as is ascertained by comparison with the steady state FTIR spectrum (Figure S3). These bleach features show no recovery over our temporal range (up to ~1 ns). A product band at 1708 $cm^{-1}$ is prominent at time delays greater than ~20 ps and remains constant in intensity until the upper limit of the probe delay range. This band is assigned to the $T_1$ state of 4TU because the band position was previously confirmed by Su and co-workers using microsecond TVAS and a molecular oxygen quenching method.[14] At early time delays (< 20 ps), there is a broad feature to the shorter wavenumber side of the $T_1$ band. The maximum of this band initially locates at 1701 $cm^{-1}$ and shifts to 1708 $cm^{-1}$, with concurrent narrowing, with a time constant of 5.2 ± 0.6 ps (Figure 1(b)). This behavior and timescale are typical of vibrational relaxation,[38] and the early time absorption is assigned to vibrationally excited

$T_1$ state molecules. The $T_1$ state populates within our effective time resolution of 0.3 ps, indicating ultrafast ISC in accord with a previous observation by TEAS.[10] A high quantum yield for the ISC is indicated by the absence of any recovery of the bleach bands on our experimental timescale. Given the reported lifetime of 230 ns for the 4TU $T_1$ state in $N_2$-saturated acetonitrile solution, no observation of ground state recovery over our temporal probe window is reasonable.[14] Careful inspection of the bleach feature at 1622 $cm^{-1}$ shows a subtle increase in depth with time, which is a result of spectral overlap with the vibrationally hot $T_1$ band at early time delays. Apart from a weak feature centered at 1439 $cm^{-1}$ showing similar time-dependence to the 1708 $cm^{-1}$ band, no further transient absorptions were observed for 4TU in the 1210 – 1760 $cm^{-1}$ region.

Our DFT calculations found two $T_1$ minima for 4TU with comparable potential energies, and infrared band intensities and wavenumbers (e.g., 1713 $cm^{-1}$ and 1721 $cm^{-1}$ for fundamental carbonyl stretching modes, see Figure S4(a) for computed infrared absorption spectra). In the case of 4TU, the close proximity of the IR bands of the two conformers prevents definitive band assignment to either or both structures.

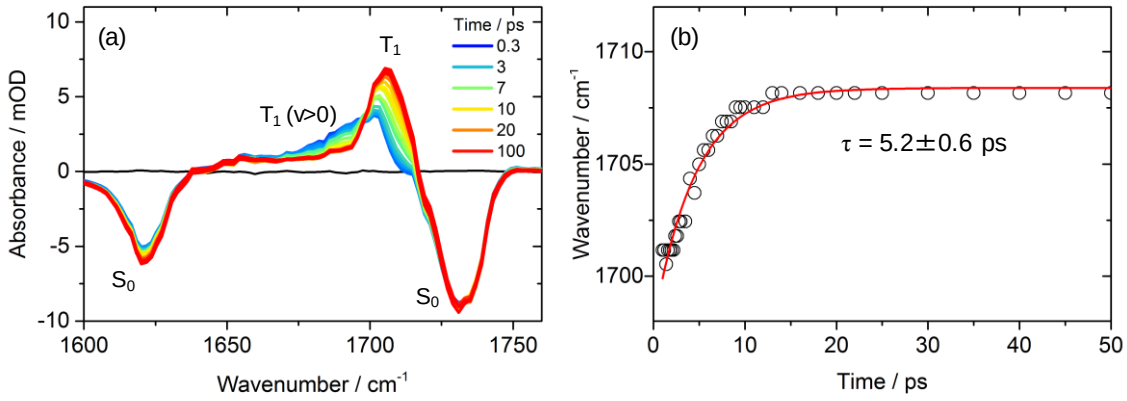

Figure 1: Triplet state population in photo-excited 4TU. (a) TVA spectra of 1.8 mM 4TU in $CD_3CN$ solution following 320-nm excitation. A TVA spectrum at negative time delay is shown in black as a baseline. (b) Time dependence of the wavenumber of the maximum of the $T_1$ band, obtained from the spectra at each time delay.

### 3.2. Photochemical Relaxation Dynamics of 2-Thiouracil

Figure 2 shows TVA spectra of 2TU in $CD_3CN$ solution following 300-nm excitation to its $S_2$ state, together with the time dependences of representative band intensities. The two most evident bleach bands at 1544 $cm^{-1}$ and 1705 $cm^{-1}$ are assigned to the parent 2TU ground state (see Figure S2 for an FTIR spectrum of 2TU). At the higher wavenumber side of the band at 1705 $cm^{-1}$, a shoulder centered at around 1720 $cm^{-1}$ can be seen both in TVAS (Figure 2(a)) and steady state FTIR (Figure S2). Previous experimental and computational studies concluded that the oxo-thione form was the predominant form of 2TU in both gas and condensed phases, and the shoulder is assigned to a combination band, instead of to another tautomeric form.[39-41] As was the case for 4TU, these parent bleach bands exhibit essentially no recovery over our temporal range. This is because of ultrafast ISC with high quantum yield to the triplet manifold, which was previously deduced from sub-picosecond and microsecond TEAS measurements, and a $T_1$ state lifetime of 70 ns in deuterated acetonitrile solution.[29,42]

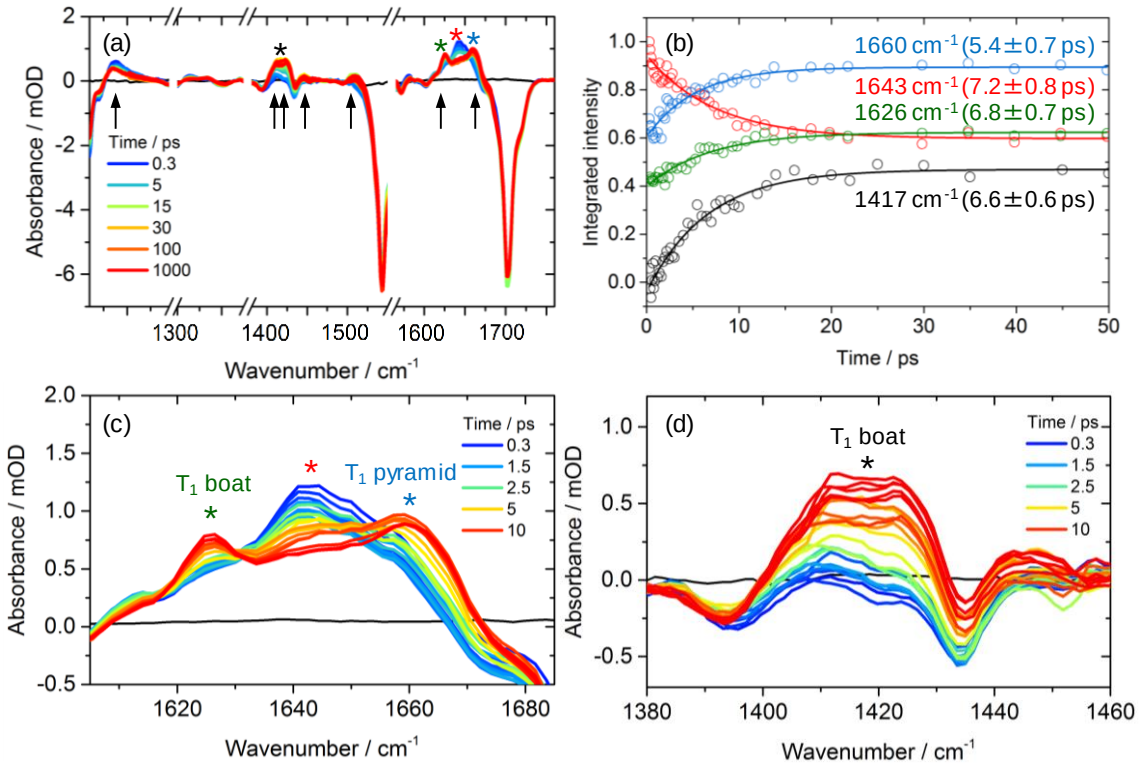


Figure 2: Transient and long-lived intermediates in the UV photochemistry of 2TU. (a) TVA spectra of 1.8 mM 2TU in $CD_3CN$ solution following 300-nm excitation. The spectra were obtained in 4 separate measurements over adjacent regions, as shown by the axis breaks. The time dependences of the integrated intensities for the bands indicated with colored asterisks are shown in (b). The product bands indicated by the arrows contribute to our assignments presented in Table 1. (c) and (d) Expanded views of the first 20 ps for the infrared regions from 1625 – 1685 $cm^{-1}$ and 1380 – 1460 $cm^{-1}$. The two bleach bands seen in (d) are parent 2TU $S_0$ bands, as ascertained by comparison with FTIR spectra presented in Figure S2.

We now focus on the various product bands. In Figure 2(a), there are seemingly six product bands centered at 1234, 1417, 1511, 1626, 1643 and 1660 $cm^{-1}$, of which the bands at 1234 and 1511 $cm^{-1}$ are spectrally overlapped with parent bleach bands. Figure 2(b) presents integrated band intensities (summed over about 5 $cm^{-1}$) for the 1417, 1626, 1643 and 1660 $cm^{-1}$ features, and Figures 2(c) and (d) provide expanded views for the

1640 $cm^{-1}$ and 1420 $cm^{-1}$ regions, respectively. The integrated intensity for the band at 1643 $cm^{-1}$ reaches its maximum within our effective time resolution of ~0.3 ps, and thereafter decays with a time constant of 7.2 ± 0.8 ps. We discuss a possible assignment of this band later. The bands at 1417, 1626 and 1660 $cm^{-1}$ grow with time constants of 5.4 ~ 6.8 ps, similar to the decaying band, and after ~20 ps remain with constant intensities until the limit of our temporal probe window of 1 ns.

Given the correspondence between the time constants for the evolution of the three spectral components in the 1620 – 1670 $cm^{-1}$ region, it is reasonable to propose that the species responsible for the band at 1643 $cm^{-1}$ is a source for the products absorbing at the slightly higher and lower wavenumbers. The kinetic traces for the bands at 1626 and 1660 $cm^{-1}$ shown in Figure 2(b) were not obtained using a full spectral decomposition of the three overlapping bands, and hence have some initial intensity which may arise from overlap with the wings of the band at 1643 $cm^{-1}$. We prefer not to present spectrally decomposed spectra and kinetics here, because the band shapes may change with time in this ultrafast regime, for example because of vibrational cooling. Global analysis, which is frequently employed for decomposition of transient absorption spectra, can be vulnerable to time-variation of band shapes and central positions,[43] and so was not attempted. Instead, we performed a different trial spectral decomposition, using the TVA spectrum at 0.3 ps as representative of the initially formed species, and the spectrum at 1000 ps for the long-lived products. With this decomposition, the 1643 $cm^{-1}$ band completely decays with a time constant of 6.6 ± 0.6 ps and the rising component evolves with a time constant of 6.1 ± 0.8 ps. Figures S5 and S6 provide examples of the spectral decomposition and resulting kinetic traces. However, this outcome must be treated with caution, because there may be an additional pathway to the long-lived products, as we

discuss later. The band centered at 1417 $cm^{-1}$ has an unusual shape, but it can be understood from the overlap of three product bands centered at 1410, 1424 and 1443 $cm^{-1}$ (see Figure S7 for an example of spectral decomposition).

Crespo-Hernández and co-workers reported ultrafast population of the 2TU $T_1$ state with a time constant of 0.3 ps in acetonitrile solution.[29] Therefore, we tested whether the observed absorption bands belong to triplet 2TU by adding styrene as a triplet energy acceptor. The outcome of these quenching studies is illustrated in Figure 3. The decays of the bands at 1626 and 1660 $cm^{-1}$ are clearly observed, as is recovery of the parent $S_0$ bleaches, indicating triplet-triplet energy transfer. Hence, the rising component in TVA spectra with a time constant of ~6 ps is assigned to the 2TU triplet state, and its lifetime of >1 ns points to the 2TU $T_1$ state.

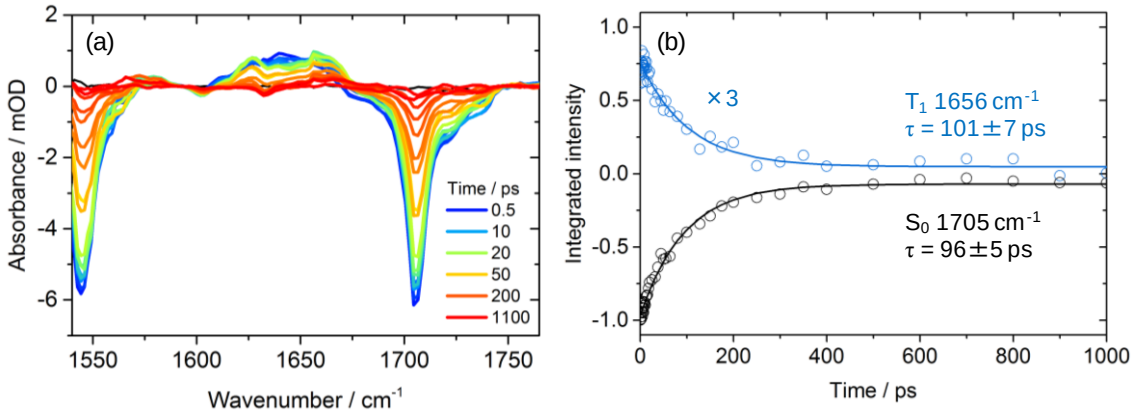


Figure 3: Quenching of the excited state of 2TU by styrene. (a) TVA spectra of 1.8 mM 2TU / 0.8 M styrene in $CD_3CN$ solution following 300-nm excitation. The small bleach band at 1632 $cm^{-1}$ corresponds to the styrene $S_0$ band. (b) Kinetic traces for the $T_1$ band at 1656 $cm^{-1}$ and the $S_0$ band at 1705 $cm^{-1}$. The integrated band intensity for the $T_1$ band is multiplied by a factor of 3 for clarity.

On the basis of their *ab initio* computational study, González and co-workers suggested the presence of two $T_1$ minima for 2TU corresponding to a boat-like structure and a structure with a pyramidal C-atom bonded to the S-atom.[23] Our DFT calculations found two similar structures, which are shown in Figure 4. These two conformers are computed to have comparable potential energies: the pyramidal structure lies 284 kJ $mol^{-1}$ above the $S_0$ equilibrium geometry, whereas the boat structure is at 280 kJ $mol^{-1}$, in reasonable accord with the previous calculations. Computed fundamental infrared frequencies and band intensities are summarized in Table 1.

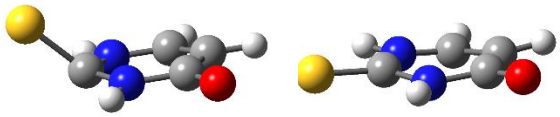


Figure 4: Equilibrium geometries for two conformers in the $T_1$ state of 2TU obtained by DFT calculations at the B3LYP / 6-311++G(3df,3pd) / CPCM (acetonitrile) level of theory. The structures are referred to in the text as pyramidal (left) and boat-like (right).

The computationally predicted infrared band positions for the boat and pyramidal $T_1$ structures are in excellent agreement with the experimental observations from TVA spectra. Both conformers must be present to account for all the observed transient absorption features. Accordingly, we assign the observed $T_1$ bands to these two conformers. The composite band centered at 1417 $cm^{-1}$ and shown in Figure 2(d) is assigned predominantly to absorptions from the boat structure because of the pronounced differences between the band intensities computed for this and the pyramidal conformer in this wavenumber region (see Table 1). The energy barrier between the two minima on the $T_1$ potential energy surface was previously suggested to be 10–12 kJ $mol^{-1}$.[23]

Hence these two conformers are expected to interchange rapidly after ISC populates the $T_1$ state, and before dissipation of any excess vibrational energy to the solvent bath.

Table 1: Computed Fundamental Infrared Band Frequencies and Intensities for Two 2TU Conformers in the $T_1$ State.

| [a] Calculation | | | | | | Experiment |
|---|---|---|---|---|---|---|
| 2TU pyramidal $T_1$ [b] 284 kJ mol$^{-1}$ | | | 2TU boat $T_1$ [b] 280 kJ mol$^{-1}$ | | | |
| Frequency /cm$^{-1}$ | Intensity /km mol$^{-1}$ | [c] Assignment | Frequency /cm$^{-1}$ | Intensity /km mol$^{-1}$ | [c] Assignment | Frequency /cm$^{-1}$ |
| 1238 | 17 | N3C4 str<br>C5H bend | 1252 | 72 | C5H bend | 1234 |
| 1319 | 42 | N1H bend<br>C6H bend | 1373 | 40 | C5H bend<br>C6H bend | [d]- |
| 1385 | 19 | N3H bend<br>C5H bend | 1403 | 384 | N1H bend<br>N3H bend | [e]1410 |
| 1440 | 10 | N3H bend | 1427 | 1037 | C6H bend | [e]1424 |
| 1495 | 64 | N1H bend<br>C6H bend | 1461 | 58 | N1H bend<br>N3H bend | [e]1443 |
| 1564 | 81 | N1H bend<br>C6H bend | 1547 | 113 | N1H bend | [f]1511 |
| 1677 | 1384 | C4O str | 1637 | 602 | C4O str | 1626, 1660 |

[a] Bands are shown in the wavenumber range of 1210–1760 cm$^{-1}$, and are compared with experimentally observed infrared band positions. Computationally predicted infrared absorption spectra are plotted in Figure S4(b).

[b] Potential energy relative to the 2TU $S_0$ minimum.

[c] Main contributor(s) to the vibrational frequency (see earlier for the ring numbering).

[d] Not observed, most likely due to weak absorption intensity.

[e] Obtained by the spectral decomposition mentioned in the main text (see Figure S7).

[f] Significantly spectrally overlapped with the parent bleach band at 1544 cm$^{-1}$ and therefore the precise band position is uncertain.

We also considered possible tautomerization in the triplet manifold because it was reported by Nowak and co-workers upon steady photo-irradiation of 2TU.[44] However, the irradiation time in their study was 2-8 hours, and the tautomer quantum yield is therefore expected to be low. Our calculations identified four tautomers and three conformers (giving a total of seven local minima) in addition to the boat and pyramidal structures of the starting tautomer of 2TU. Further details are provided in the Supporting Information and Table S3, but we discounted these as significant photoproducts on the basis of their computed energies and infrared frequencies.

Finally, we concentrate on assignment of the band at 1643 $cm^{-1}$, which decays with a time constant of 7.2 ps. There are two reasonable candidates: the vibrationally excited $T_1$ state, or molecules in the $S_1$ state. Any assignment must also be compatible with the 0.3 ps time constant for population of the $T_1$ state deduced from the TEAS studies by Crespo-Hernández and coworkers.[29]

The first candidate is plausible if the $T_1$ state is initially populated from the higher-lying $S_2$ or $S_1$ states on sub-picosecond timescales, because the time constant for decay of the 1643 $cm^{-1}$ feature is similar to that for vibrational relaxation of $T_1$-state 4TU in $CD_3CN$ (Figure 1). We do not observe the usual behavior of a band shift to higher wavenumber associated with anharmonic vibrational modes, but this may be a consequence of a PES with a double minimum, and overlap with the growing features to either side at 1626 and 1660 $cm^{-1}$ as excess vibrational energy is transferred to the solvent bath. However, as seen in Figure 2(d), the band at 1417 $cm^{-1}$ (comprising several contributions all assigned to boat-conformer $T_1$ molecules) also does not show any clear evidence of decay of vibrationally excited molecules (i.e., a band shift to the higher

wavenumber side, with concurrent narrowing).

We consider the second candidate assignment within the context of calculations by González and co-workers, which examined three relaxation pathways for the population of the 2TU $T_1$ state using *ab initio* dynamics simulations: (i) $S_2 \rightarrow S_1 \rightarrow T_2 \rightarrow T_1$; (ii) $S_2 \rightarrow S_1 \rightarrow T_1$; and (iii) $S_2 \rightarrow T_2$ (or $T_3$) $\rightarrow T_1$, with respective contributions of 40, 35 and 25% to the $T_1$ population.[24] Assuming that depopulation of the $S_2$ state is ultrafast (less than 100 fs),[21, 24] the sub-ps population of the $T_1$ state seen by TEAS,[29] and the 7-ps decay of the 1643 $cm^{-1}$ band reported here can be explained by these proposed pathways if IC of the $T_2$ (or $T_3$) state to the $T_1$ state accounts for the 0.3 ps population of $T_1$ via pathway (iii), and the 7-ps time constant corresponds to ISC from the $S_1$ state to the $T_2$ or $T_1$ states (pathways (i) and (ii)). The reverse assignment of the time constants is kinetically possible, but suggests $T_2 \rightarrow T_1$ IC is an order of magnitude slower than the dynamics simulations predict, and is deemed less likely unless the accessibility of the $T_2/T_1$ conical intersections is significantly modified by the solvent. Our TDDFT calculations found two conformers in the $S_1$ state, with an almost planar and a pyramidal structure and comparable potential energies (see the Supporting Information). Both structures are similar to previous predictions,[23, 26] and are computed to have an infrared absorption either at 1654 $cm^{-1}$ (for the planar structure) or 1678 $cm^{-1}$ (for the pyramidal structure), with large band intensities (Table S2). The agreement between these calculated band positions and the experimentally observed transient feature at 1643 $cm^{-1}$ justifies our consideration of the second proposed assignment to $S_1$-state molecules.

Population of the $T_1$ state on a sub-picosecond timescale, as well as via a slower route, suggests that signatures of the $T_1$ bands should be evident in our earliest TVA

spectra. At a time delay of 0.3 ps, the absorbance is almost zero for the band at 1410 $cm^{-1}$ in Figure 2(d), and slightly negative for the band at 1424 $cm^{-1}$. However, these bands are spectrally overlapped with the parent bleach features (see the FTIR spectrum in Figure S7), and contribute roughly 30% of the absorbance at a time delay of 0.3 ps according to our spectral decomposition. Hence the second interpretation of our data cannot be discounted on the basis of this experimental evidence.

Sánchez-Rodríguez *et al*. recently presented further arguments based on TEAS measurements of 2TU in acetonitrile for ISC occurring from the $S_1$ state with a sub-ps time constant, and subsequent vibrational cooling in the $T_1$ state on a timescale of a few ps. They also attributed the observed longer-time decay behavior of the $T_1$ state population to the presence of the two minima corresponding to distinct conformers of this triplet state.[17] If the interpretation of their TEA measurements is correct and complete, we can rule out transient population of the $S_1$ state (perhaps with some vibrational cooling) as responsible for the ~7-ps decay of the 1643 $cm^{-1}$ band, and instead assign this feature to vibrationally excited $T_1$-state population, much as we observe for 4TU.

## CONCLUSIONS

The relaxation dynamics of 2TU and 4TU in $CD_3CN$ solutions have been investigated after photoexcitation to their $S_2$ states, using sub-picosecond transient vibrational absorption spectroscopy. Following 320-nm excitation, vibrationally excited population of the 4TU $T_1$ state is seen within the effective time resolution of 0.3 ps, with a time constant of 5.2 ± 0.6 ps for vibrational relaxation. No recovery of the 4TU $S_0$

bands is observed, which is consistent with the high quantum yield for ISC reported previously.[14]

Evidence from TVA spectra of 2TU photoexcited at 300 nm points to population of two different conformers in the $T_1$ state, as proposed recently from computational studies.[25] The absorption bands of these two species grow with time constants of 7.2 ± 0.8 ps, and develop either side of a band at 1643 $cm^{-1}$ which decays on the same timescale. The 1643 $cm^{-1}$ band is evident with its maximum intensity at the earliest time delay (0.3 ps) in our experimental measurements, and two assignments are considered: (a) vibrationally hot $T_1$ molecules, produced by ultrafast ISC from the $S_2$ or $S_1$ states, with initial energies above the barrier for conformational exchange; (b) $S_1$ state molecules, produced by ultrafast internal conversion from the $S_2$ state, which decay by intersystem crossing to the triplet manifold. We cannot definitively differentiate between these two interpretations, but the former assignment is consistent with the interpretation of previous studies which argued that ISC from the $S_1$ state takes place on a sub-picosecond timescale.[17, 24, 29] The parent 2TU $S_0$ bands do not show any recovery over our temporal probe window of 1 ns, indicating a high quantum yield for ISC in this, as well as 4-thiouracil.

## ELECTRONIC SUPPORTING INFORMATION AVAILABLE

Supporting Information. Steady state UV/vis absorption and FTIR spectra of 2TU and 4TU; examples of spectral decompositions and kinetic traces for the decomposed spectra; computed infrared frequencies for tautomers and conformers in the 2TU $T_1$ and $S_1$ states;

TVA spectra of 2TU following 320-nm excitation.

All experimental data are archived in the University of Bristol's Research Data Storage Facility (DOI: 10.5523/bris.2luw7dg6n57uk2rad5ot4k79w4).

ACKNOWLEDGEMENTS

We thank the European Research Council (ERC, Advanced Grant 290966 CAPRI) for financial support.

REFERENCES

1. Improta, R.; Santoro, F.; Blancafort, L., Quantum Mechanical Studies on the Photophysics and the Photochemistry of Nucleic Acids and Nucleobases. *Chem. Rev.* **2016**, *116*, 3540-3593.
2. Crespo-Hernández, C. E.; Hare, P. M.; Cohen, B.; Kohler, B., Ultrafast Excited-State Dynamics in Nucleic Acids. *Chem. Rev.* **2004**, *104*, 1977-2019.
3. Middleton, C. T.; de La Harpe, K.; C., S.; K., L. Y.; Crespo-Hernández, C. E.; Kohler, B., DNA Excited-State Dynamics: From Single Bases to the Double Helix. *Annu. Rev. Phys. Chem.* **2009**, *60*, 217-239.
4. Carell, T.; Brandmayr, C.; Hienzsch, A.; Müller, M.; Pearson, D.; Reiter, V.; Thoma, I.; Thumbs, P.; Wagner, M., Structure and Function of Noncanonical Nucleobases. *Angew. Chem., Int. Ed.* **2012**, *51*, 7110-7131.
5. Komeda, K.; Iwamoto, S.; Kominami, S.; Ohnishi, T., Induction of Cell Killing, Mutation and umu Gene Expression by 6-Mercaptopurine or 2-Thiouracil with UVA Irradiation. *Photochem. Photobiol.* **1997**, *65*, 115-118.
6. Sochacka, E.; Kraszewska, K.; Sochacki, M.; Sobczak, M.; Janicka, M.; Nawrot, B., The 2-Thiouridine Unit in the RNA Strand is Desulfured Predominantly to 4-Pyrimidinone Nucleoside under in vitro Oxidative Stress Conditions. *Chem. Commun.* **2011**, *47*, 4914-4916.
7. Reelfs, O.; Karranb, P.; Younga, A. R., 4-Thiothymidine Sensitization of DNA

to UVA Offers Potential for a Novel Photochemotherapy. *Photochem. Photobiol. Sci.* **2012**, *11*, 148-154.

8. Reichardt, C.; Guo, C.; Crespo-Hernández, C. E., Excited-State Dynamics in 6-Thioguanosine from the Femtosecond to Microsecond Time Scale. *J. Phys. Chem. B* **2011**, *115*, 3263.

9. Pollum, M.; Jockusch, S.; Crespo-Hernández, C. E., 2,4-Dithiothymine as a Potent UVA Chemotherapeutic Agent. *J. Am. Chem. Soc.* **2014**, *136*, 17930-17933.

10. Pollum, M.; Jockusch, S.; Crespo-Hernández, C. E., Increase in the Photoreactivity of Uracil Derivatives by Doubling Thionation. *Phys. Chem. Chem. Phys.* **2015**, *17*, 27851-27861.

11. Mai, S.; Pollum, M.; Martínez-Fernández, L.; Dunn, N.; Marquetand, P.; Corral, I.; Crespo-Hernández, C. E.; González, L., The Origin of Efficient Triplet State Population in Sulfur-Substituted Nucleobases. *Nature Commun.* **2016**, *7*, 13077.

12. Harada, Y.; Okabe, C.; Kobayashi, T.; Suzuki, T.; Ichimura, T.; Nishi, N.; Xu, Y., Ultrafast Intersystem Crossing of 4-Thiothymidine in Aqueous Solution. *J. Phys. Chem. Lett.* **2010**, *1*, 480-484.

13. Kuramochi, H.; Kobayashi, T.; Suzuki, T.; Ichimura, T., Excited-State Dynamics of 6-Aza-2-thiothymine and 2-Thiothymine: Highly Efficient Intersystem Crossing and Singlet Oxygen Photosensitization. *J. Phys. Chem. B* **2010**, *114*, 8782-8789.

14. Zou, X.; Dai, X.; Liu, K.; Zhao, H.; Song, D.; Su, H., Photophysical and Photochemical Properties of 4-Thiouracil: Time-Resolved IR Spectroscopy and DFT Studies. *J. Phys. Chem. B* **2014**, *118*, 5864-5872.

15. Taras-Goślińska, K.; Burdziński, G.; Wenska, G., Relaxation of the T1 Excited State of 2-Thiothymine, its Riboside Anddeoxyriboside-Enhanced Nonradiative Decay Rate Induced by Sugarsubstituent. *J. Photochem. Photobiol., A* **2014**, *275*, 89-95.

16. Martínez-Fernández, L.; Granucci, G.; Pollum, M.; Crespo-Hernández, C. E.; Persico, M.; Corral, I., Decoding the Molecular Basis for the Population Mechanism of the Triplet Phototoxic Precursors in UVA Light-Activated Pyrimidine Anticancer Drugs. *Chem. Eur. J.* **2017**, *23*, 2619-2627.

17. Sánchez-Rodríguez, J. A.; Mohamadzade, A.; Mai, S.; Ashwood, B.; Pollum, M.; Marquetand, P.; González, L.; Crespo-Hernández, C. E.; Ullrich, S., 2-Thiouracil Intersystem Crossing Photodynamics Studied by Wavelength-Dependent Photoelectron and Transient Absorption Spectroscopies. *Phys. Chem. Chem. Phys.* **2017**, *19*, 19756-19766.

18. Martínez-Fernández, L.; González, L.; Corral, I., An Ab Initio Mechanism for Efficient Population of Triplet States in Cytotoxic Sulfur Substituted DNA Bases: the

Case of 6-Thioguanine. *Chem. Commun.* **2012**, *48*, 2134-2136.
19. Cui, G.; Fang, W., State-Specific Heavy-Atom Effect on Intersystem Crossing Processes in 2-Thiothymine: A Potential Photodynamic Therapy Photosensitizer. *J. Chem. Phys.* **2013**, *138*, 044315.
20. Martínez-Fernández, L.; Corral, I.; Granucci, G.; Persico, M., Competing Ultrafast Intersystem Crossing and Internal Conversion: A Time Resolved Picture for the Deactivation of 6-Thioguanine. *Chem. Sci.* **2014**, *5*, 1336-1347.
21. Jiang, J.; Zhang, T.; Xue, J.; Zheng, X.; Cui, G.; Fang, W., Short-Time Dynamics of 2-Thiouracil in the Light Absorbing S2(ππ*) State. *J. Chem. Phys.* **2015**, *143*, 175103.
22. Ruckenbauer, M.; Mai, S.; Marquetand, P.; González, L., Photoelectron Spectra of 2-Thiouracil, 4-Thiouracil and 2,4-Dithiouracil. *J. Chem. Phys.* **2015**, *144*, 074303.
23. Mai, S.; Marquetand, P.; González, L., A Static Picture of the Relaxation and Intersystem Crossing Mechanisms of Photoexcited 2-Thiouracil. *J. Phys. Chem. A* **2015**, *119*, 9524.
24. Mai, S.; Marquetand, P.; González, L., Intersystem Crossing Pathways in the Noncanonical Nucleobase 2-Thiouracil: A Time-Dependent Picture. *J. Phys. Chem. Lett.* **2016**, *7*, 1978-1983.
25. Bai, S.; Barbatti, M., On the Decay of the Triplet State of Thionucleobases. *Phys. Chem. Chem. Phys.* **2017**, *19*, 12674-12682.
26. Gobbo, J. P.; Borin, A. C., 2-Thiouracil Deactivation Pathways and Triplet States Population. *Comput. Theor. Chem.* **2014**, *1040-1041*, 195-201.
27. Pollum, M.; Martínez-Fernández, L.; Crespo-Hernández, C. E., Photochemistry of Nucleic Acid Bases and their Thio- and Aza-Analogues in Solution. *Top. Curr. Chem.* **2015**, *355*, 245-327.
28. Arslancan, S.; Martínez-Fernández, L.; Corral, I., Photophysics and Photochemistry of Canonical Nucleobases' Thioanalogs: From Quantum Mechanical Studies to Time Resolved Experiments. *Molecules* **2017**, *22*, 998.
29. Pollum, M.; Crespo-Hernández, C. E., The Dark Singlet State as a Doorway State in the Ultrafast and Efficient Intersystem Crossing Dynamics in 2-Thiothymine and 2-Thiouracil. *J. Chem. Phys.* **2014**, *140*, 071101.
30. Koyama, D.; Orr-Ewing, A. J., Triplet State Formation and Quenching Dynamics of 2-Mercaptobenzothiazole in Solution. *Phys. Chem. Chem. Phys.* **2016**, *18*, 26224-26235.
31. Roberts, G. M.; Marroux, H. J. B.; Grubb, M. P.; Ashfold, M. N. R.; Orr-Ewing, A. J., On the Participation of Photoinduced N−H Bond Fission in Aqueous Adenine at 266 and 220 nm: A Combined Ultrafast Transient Electronic and Vibrational Absorption

Spectroscopy Study. *J. Phys. Chem. A* **2014**, *118*, 11211-11225.
32. Röttger, K.; Marroux, H. J. B.; Böhnke, H.; Morris, D. T. J.; Voice, A. T.; Temps, F.; Roberts, G. M.; Orr-Ewing, A. J., Probing the Excited State Relaxation Dynamics of Pyrimidine Nucleosides in Chloroform Solution. *Faraday Discussions* **2016**, *194*, 683-708.
33. Frisch, M. J.; Trucks, G. W.; Schlegel, H. B.; Scuseria, G. E.; Robb, M. A.; Cheeseman, J. R.; Scalmani, G.; Barone, V.; Mennucci, B.; Petersson, G. A., et al., *Gaussian 09*, Gaussian Inc., Wallingford CT **2009**.
34. Lee, C.; Yang, W.; Parr, R. G., Development of the Colle-Salvetti Correlation-Energy Formula into a Functional of the Electron Density. *Phys. Rev. B* **1988**, *37*, 785-789.
35. Becke, A. D., Densityfunctional Thermochemistry. III. The Role of Exact Exchange. *J. Chem. Phys.* **1993**, *98*, 5648-5652.
36. Barone, V.; Cossi, M., Quantum Calculation of Molecular Energies and Energy Gradients in Solution by a Conductor Solvent Model. *J. Phys. Chem. A* **1998**, *102*, 1995-2001.
37. Cossi, M.; Rega, N.; Scalmani, G.; Barone, V., Energies, Structures, and Electronic Properties of Molecules in Solution with the C-PCM Solvation Model. *J. Comp. Chem.* **2003**, *24*, 669-681.
38. Murdock, D.; Ingle, R. A.; Sazanovich, I. V.; Clark, I. P.; Harabuchi, Y.; Taketsugu, T.; Maeda, S.; Orr-Ewing, A. J.; Ashfold, M. N. R., Contrasting Ring-Opening Propensities in UV-Excited α-Pyrone and Coumarin. *Phys. Chem. Chem. Phys.* **2016**, *18*, 2629-2638.
39. Rostkowska, H.; Szczepaniak, K.; Nowak, M. J.; Leszczynski, J.; KuBulat, K.; Person, W. B., Thiouracils. 2. Tautomerism and Infrared Spectra of Thiouracils. Matrix-Isolation and Ab Initio Studies. *J. Am. Soc. Chem.* **1990**, *112*, 2147-2160.
40. Shukla, M. K.; Leszczynski, J., Electronic Transitions of Thiouracils in the Gas Phase and in Solutions: Time-Dependent Density Functional Theory (TD-DFT) Study. *J. Phys. Chem. A* **2004**, *108*, 10367-10375.
41. Puzzarini, C.; Biczysko, M.; Barone, V.; Peña, I.; Cabezas, C.; Alonso, J. L., Accurate Molecular Structure and Spectroscopic Properties of Nucleobases: A Combined Computational - Microwave Investigation of 2-Thiouracil as a Case Study. *Phys. Chem. Chem. Phys.* **2013**, *15*, 16965-16975.
42. Vendrell-Criado, V.; Sáez, J. A.; Lhiaubet-Vallet, V.; Cuquerella, M. C.; Miranda, M. A., Photophysical Properties of 5-Substituted 2-Thiopyrimidines. *Photochem. Photobiol. Sci.* **2013**, *12*, 1460-1465.

43. Marciniak, H.; Lochbrunner, S., On the Interpretation of Decay Associated Spectra in the Presence of Time Dependent Spectral Shifts. *Chem. Phys. Lett.* **2014**, *609*, 184-188.
44. Khvorostov, A.; Lapinski, L.; Rostkowska, H.; Nowak, M. J., UV-Induced Generation of Rare Tautomers of 2-Thiouracils: A Matrix Isolation Study. *J. Phys. Chem. A* **2005**, *109*, 7700-7707.

TOC Graphic